Journal of Virology

Tempo and Mode of Plant RNA Virus Escape from RNA Interference-Mediated Resistance

Guillaume Lafforgue, Fernando Martínez, Josep Sardanyés, Francisca de la Iglesia, Qi-Wen Niu, Shih-Shun Lin, Ricard V. Solé, Nam-Hai Chua, José-Antonio Daròs and Santiago F. Elena

J. Virol. **2011, 85(19):9686. DOI: 10.1128/JVI.05326-11. Published Ahead of Print 20 July 2011.**

JOURNAL OF VIROLOGY, Oct. 2011, p. 9686–9695 Vol. 85, No. 19
0022-538X/11/$12.00 doi:10.1128/JVI.05326-11

Tempo and Mode of Plant RNA Virus Escape from RNA Interference-Mediated Resistance▽

Guillaume Lafforgue,[1]† Fernando Martínez,[1]† Josep Sardanyés,[1]† Francisca de la Iglesia,[1] Qi-Wen Niu,[2] Shih-Shun Lin,[2]§ Ricard V. Solé,[3,4,5] Nam-Hai Chua,[2] José-Antonio Daròs,[1] and Santiago F. Elena[1,5]*

Instituto de Biología Molecular y Celular de Plantas, Consejo Superior de Investigaciones Científicas-Universitat Politècnica de València, València, Spain[1]; Laboratory of Plant Biology, Rockefeller University, New York, New York[2]; Complex Systems Laboratory, ICREA-Universitat Pompeu Fabra, Barcelona, Spain[3]; Instituto de Biología Evolutiva, Universitat Pompeu Fabra-Consejo Superior de Investigaciones Científicas, Barcelona, Spain[4]; and The Santa Fe Institute, Santa Fe, New Mexico[5]

Received 7 June 2011/Accepted 12 July 2011

A biotechnological application of artificial microRNAs (amiRs) is the generation of plants that are resistant to virus infection. This resistance has proven to be highly effective and sequence specific. However, before these transgenic plants can be deployed in the field, it is important to evaluate the likelihood of the emergence of resistance-breaking mutants. Two issues are of particular interest: (i) whether such mutants can arise in nontransgenic plants that may act as reservoirs and (ii) whether a suboptimal expression level of the transgene, resulting in subinhibitory concentrations of the amiR, would favor the emergence of escape mutants. To address the first issue, we experimentally evolved independent lineages of *Turnip mosaic virus* (TuMV) (family *Potyviridae*) in fully susceptible wild-type *Arabidopsis thaliana* plants and then simulated the spillover of the evolving virus to fully resistant *A. thaliana* transgenic plants. To address the second issue, the evolution phase took place with transgenic plants that expressed the amiR at subinhibitory concentrations. Our results show that TuMV populations replicating in susceptible hosts accumulated resistance-breaking alleles that resulted in the overcoming of the resistance of fully resistant plants. The rate at which resistance was broken was 7 times higher for TuMV populations that experienced subinhibitory concentrations of the antiviral amiR. A molecular characterization of escape alleles showed that they all contained at least one nucleotide substitution in the target sequence, generally a transition of the G-to-A and C-to-U types, with many instances of convergent molecular evolution. To better understand the viral population dynamics taking place within each host, as well as to evaluate relevant population genetic parameters, we performed *in silico* simulations of the experiments. Together, our results contribute to the rational management of amiR-based antiviral resistance in plants.

The natural function of plant microRNAs (miRNAs) is to regulate the abundance of target mRNAs by guiding the RNA-induced silencing complex (RISC) to cleave the corresponding complementary sequence. It has also been shown that changes within the miRNA 21-nucleotide (nt) sequence do not affect its biogenesis and maturation (24, 46), and this finding opened up the possibility for a redesigning of the miRNA sequence to target different transcripts using different pre-miRNAs as backbones (38, 39, 50). One of the many applications of this technology is to produce artificial miRNAs (amiRs) targeting viral genomes, thus generating transgenic plants that are resistant to viral infection (38, 39). Niu et al. (38) previously used the pre-miRNA159a precursor to express two amiR159s with sequences complementary to the RNA genomes of *Turnip yellow mosaic virus* (TYMV) and of *Turnip mosaic virus* (TuMV), respectively. amiR159-P69 was designed to target the sequence of the P69 silencing suppressor protein of TYMV. Similarly, amiR159-HCPro was designed to target the sequence of the TuMV silencing suppressor HC-Pro. The transgenic expression of the amiRs conferred high levels of specific resistance to the corresponding virus.

Similar to the case of virus-resistant transgenic plants, a gene-silencing mechanism (RNA interference [RNAi]) has been used in *in vitro* assays as an antiviral therapeutic to inhibit the replication of several human viruses, including human immunodeficiency virus type 1 (12), hepatitis C virus (30), and influenza A virus (22). A major issue confronting these *in vitro* assays with mammalian viruses, however, has been the emergence of resistance variants (4, 17, 23, 52). These variants differ from the wild-type (WT) virus by one or more point mutations in the 21-nt target sequence leading to imperfect matching and, hence, not being properly or efficiently processed by the RISC (40, 48, 52). The RNAi machinery tolerates changes in certain positions of the 21-nt target but is particularly sensitive to changes in the central positions (particularly positions 9 and 11) (19, 51). Lin et al. (31) extended these observations to the case of plant viruses. By use of transgenic *Arabidopsis thaliana* plants expressing amiR159-P69 described above and an engi-

* Corresponding author. Mailing address: IBMCP (CSIC-UPV), Campus UPV CPI 8E, Ingeniero Fausto Elio s/n, 46022 València, Spain. Phone: 34 963 877 895. Fax: 34 963 877 859. E-mail: sfelena@ibmcp.upv.es.

† G.L., F.M., and J.S. contributed equally to this study.

§ Present address: Institute of Biotechnology, National Taiwan University, Taipei, Taiwan.

▽ Published ahead of print on 20 July 2011.

neered version of TuMV that carried an insert corresponding to the 21-nt TYMV P69 target, it was shown that the conservation of positions 3 to 6, 9, and 12 was absolutely essential for the RISC to cleave the viral genome; changes in positions 2, 10, 11, 13, 15, and 18 had a moderate effect on the cleavage efficiency, whereas changes in the remaining nine positions had very minor effects on the processing efficiency (31). Furthermore, when viruses mutated at every one of the 21-nt targets were allowed to replicate in the amiR159-P69 transgenic plants, deletions of variable lengths or additional changes at alternative sites arose and increased in frequency in the viral population, further jeopardizing the resistance of the transgenic plants (31). It is important that in this experiment, the 21-nt target was noncoding; thus, selection operated only at the RNA level and was not constrained by protein-coding requirements.

Altogether, these results demonstrated that changes in certain sites within the 21-nt target may generate virus escape variants. However, the relevance, if any, of these escape variants in natural viral populations remains to be established. In other words, to evaluate the viability of antiviral therapies based on the transgenic expression of amiRs in crops, it is essential to evaluate the likelihood of viral populations infecting susceptible reservoir host species to contain escape variants that may be subsequently transmitted to the transgenic crops by vectors. Moreover, it is also pivotal to evaluate whether variations in the expression of the amiR transgenes, especially at subinhibitory concentrations, would affect the accumulation and evolution of escape viral mutants. More specifically, we are interested in addressing the following issues. What is the likelihood of escape mutations arising and accumulating in a WT host population? Does partial resistance favor the accumulation of escape mutants? What sites in the 21-nt target are more critical for escape from RNAi surveillance? What are the basic population genetic parameters governing the escape process? To address these issues, we performed two sets of evolution experiments together with their corresponding *in silico* simulations. In the first set, 25 independent TuMV populations evolving in fully susceptible WT *A. thaliana* plants were periodically tested for the presence of escape mutants by challenging fully resistant *A. thaliana* plants (Fig. 1A). We observed a steady increase in the number of evolving lineages able to break the resistance. The second set of experiments was similar to the first set, except that 25 independent TuMV populations were evolved in partially susceptible *A. thaliana* plants expressing subinhibitory concentrations of amiR159-HCPro. We found that resistance breaking occurred faster in the second experiment. In all cases, changes in the 21-nt target sequence were observed. These results show that escape variants maintained at a low frequency in sensitive and partially resistant transgenic plants were quickly filtered out upon transmission to fully resistant transgenic plants. The *in silico* simulation algorithm was used to evaluate population genetic parameters governing the evolutionary dynamics of escape mutants.

MATERIALS AND METHODS

Plant material and growth conditions. Two transgenic *A. thaliana* Col-0 lines expressing amiR159-HCPro were used in this study: 10-4 and 12-4 (38). Seeds corresponded to homozygous T4 generations. Plants were maintained in a growth chamber under conditions of 16 h of light at 25°C and 8 h of darkness at 22°C.

Quantification of amiR159-HCPro expression. Total RNA was extracted and purified from *A. thaliana* tissue by use of TRIzol reagent (Invitrogen). RNA was precipitated with isopropanol, resuspended in H_2O, and quantified by spectrophotometry. The quantification of amiR159-HCPro in RNA preparations was performed by reverse transcriptase (RT) quantitative PCR (qPCR) in triplicate (45). Standards were prepared by the addition of known amounts of the synthetic oligoribonucleotide 5′-r(ACUUGCUCACGCACUCGACUG)-3′, corresponding in sequence to amiR159-HCPro, to a nontransgenic *A. thaliana* total RNA preparation. RT reactions were done with a 10-μl mixture containing 100 ng total RNA, 1 pmol primer I (PI) (5′-GTCGTATCCAGTGCAGGGTCCGAGGTATTCGCACTGGATACGAC**CAGTCG**-3′ [the sequence complementary to amiR159-HCPro is in boldface type]), and 30 U Moloney murine leukemia virus (M-MuLV) RT (Fermentas), with incubation for 10 min at 25°C, 45 min at 42°C, 10 min at 50°C, 5 min at 60°C, and, finally, 15 min at 70°C. qPCR was done with a 20-μl mixture containing 2 μl of RT reaction mix and 10 pmol each primer PII (5′-CGGCGG**ACTTGCTCACGCACT**-3′ [the sequence complementary to amiR159-HCPro is in boldface type]) and PIII (5′-GTGCAGGGTCCGAGGT-3′ [homologous to the sequence underlined in PI]) with Maxima SYBR green master mix (Fermentas) and incubation for 10 min at 95°C, followed of 40 cycles of 15 s at 95°C, 30 s at 60°C, and 30 s at 72°C.

Population passages and evaluation of pathogenicity in *A. thaliana* 12-4 plants. As a source of the TuMV inoculum for all our experiments, we used a large stock of infectious sap obtained from TuMV-infected *Nicotiana benthamiana* plants inoculated with a plasmid containing TuMV cDNA (GenBank accession no. AF530055.2) under the control of the *Cauliflower mosaic virus* 35S promoter. This TuMV sequence variant corresponds to isolate YC5 from calla lily (*Zantedeschia* sp.) (10). Plant infectious saps were obtained by grinding the infected tissue in a mortar with 20 volumes of grinding buffer (50 mM potassium phosphate [pH 7.0], 3% polyethylene glycol 6000 [PEG 6000]).

Figure 1A summarizes the experimental design for the evolution experiments. Aliquots of 5 μl of 10% Carborundum in grinding buffer were applied onto three different *A. thaliana* leaves, and inoculation was done mechanically by gentle rubbing with a cotton swab soaked with infectious sap. Twenty-five WT *A. thaliana* and 25 10-4 transgenic plants were initially inoculated. Each plant represented the starting point for an independent evolution lineage. At 14 days postinfection (dpi), symptomatic tissue was collected for each lineage and homogenized in grinding buffer. A portion of the resulting saps was used to inoculate the next set of plants. A second portion of the homogenized sap was frozen at −80°C for further characterization. The remaining portion was used for the challenge experiments designed to estimate pathogenicity in 12-4 plants. This procedure was repeated until all 50 evolutionary lineages overcame the resistance of the 12-4 line. Once a lineage was capable of breaking resistance, it was removed from the passaging experiment.

For the pathogenicity test experiments, 20 plants of the 12-4 line were inoculated as described above. Plants were visually checked for the presence of symptoms at 14 dpi, and the frequency of infected plants, that is, pathogenicity, was recorded. These challenge experiments were performed after every evolutionary passage for each one of the 50 evolving lineages. A pilot experiment showed that infection always concurred with symptom development. A lineage was considered to be capable of breaking resistance if at least one 12-4 plant showed symptoms.

Sequence analysis of the 21-nt target region. The region around the 21-nt target of amiR159-HCPro was sequenced in virus populations breaking resistance. Total RNA from infected *A. thaliana* 12-4 transgenic plants was purified by use of silica columns (Zymo Research), and a viral cDNA was amplified by RT-PCR. RT reactions were carried out with a 10-μl solution containing 50 μl M-MuLV RT and 5 pmol primer IV (5′-CCTGGTGACAGTAAAGCATATAATGG-3′) for 45 min at 42°C, 5 min at 50°C, and 5 min at 60°C. One microliter of the RT reaction was used for PCR amplification in a 20-μl mixture with 0.4 U Phusion DNA polymerase (Finnzymes) and 10 pmol each primer PV (5′-GACAATGAGTCACAAGATTGTGCACTTT-3′) and PVI (5′-CATGAGTGTCCTCCCATTCTGTCCC-3′), with incubation for 30 s at 98°C; 30 cycles of 10 s at 98°C, 30 s at 55°C, and 30 s at 72°C; and a final extension step for 10 min at 72°C. Amplification products were separated by electrophoresis in a 1% agarose gel, and the TuMV cDNAs matching the expected 1,427 bp were eluted and sequenced with primer PVII (5′-AAACGATTCTTCAGCAACTACTTTG-3′).

Simulation algorithm. The experiments were simulated by using a bit-string Monte Carlo model (20, 34), in which digital genomes were represented by binary strings, ***S***, of a length, *L*, of 31 bits. The digital genomes explicitly considered the 21 nt of the amiR159-HCPro target and added 10 more bits, each corresponding to one of the 10 viral cistrons (Fig. 1B). We made this distinction

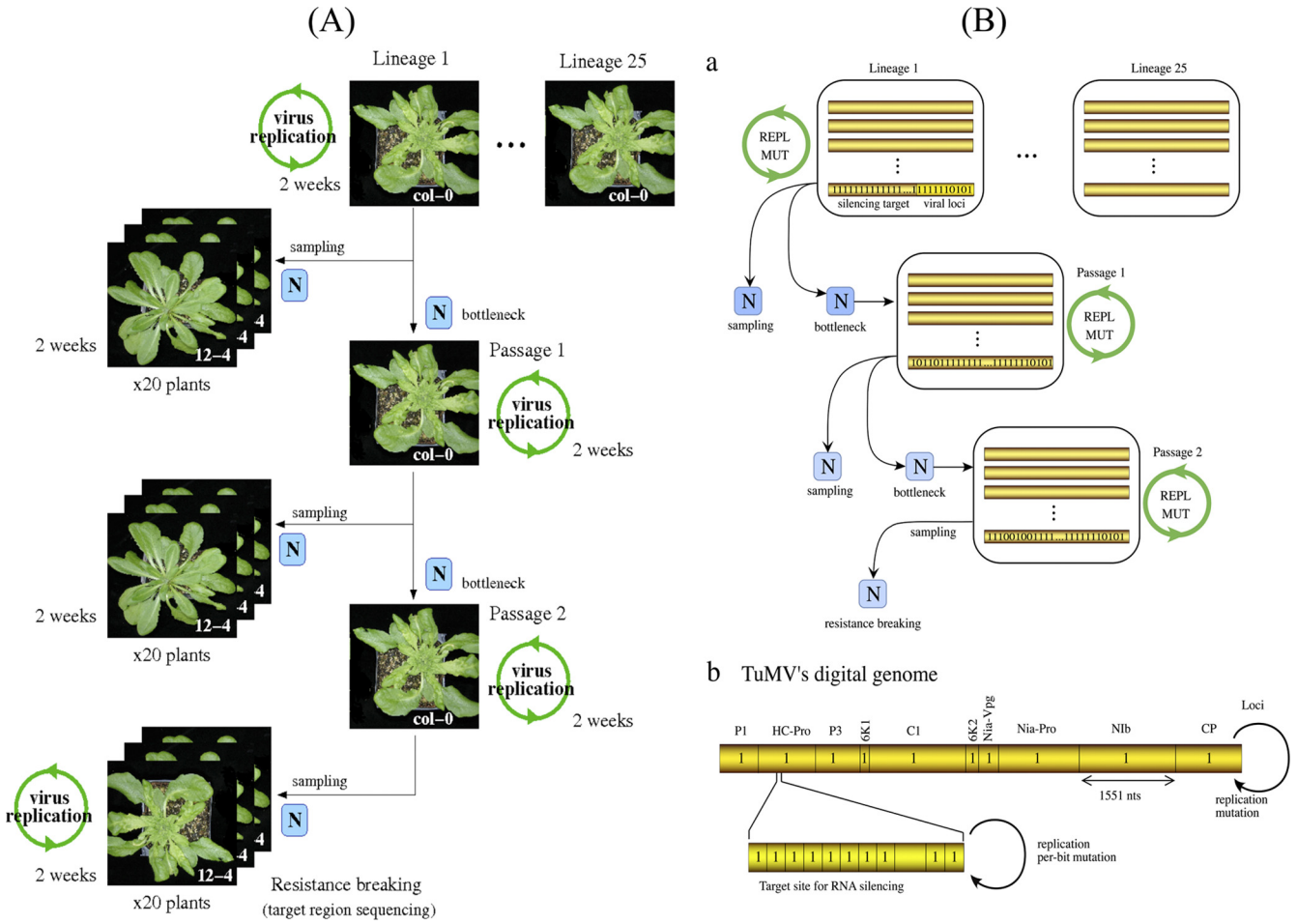

FIG. 1. (A) Schematic representation of the experimental design. For illustrative purposes we show only one of the WT *A. thaliana*-evolved lineages. The same protocol was repeated for the 10-4 lineages, with the exception that serial passages were performed on *A. thaliana* 10-4 transgenic plants. In the illustrated example, resistance breaking occurred at passage 2 (note symptoms in the corresponding 12-4 plants). (B) Schematic diagram of the *in silico* simulation model. (a) Each lineage was considered a population of bit-strings containing the 21 bits of the target region plus 10 loci, each corresponding to the different cistrons in the TuMV genome. The model simulated within-host viral replication with mutation and bottleneck transmission between passages. For the simulations of virus evolution in WT *A. thaliana* plants, we did not consider target-specific degradation of strings, while for simulating the evolution in 10-4 plants, we included a degradation probability, ε, for strings with a WT target sequence. (b) Digital genome of TuMV where the target sequence has been explicitly considered.

to disentangle the effects due to a mutation in the target (evaluated at the challenge step of the experiment) from those associated with changes in other viral genes and that determine the overall fitness of the virus. The maximum string population size was set to an N_{max} of 5,000 genomes. As in the experiments, the simulation model considered 25 independent lineages (Fig. 1B). Each lineage started with a sample of size $N < N_{max}$ of WT genomes. For each lineage we let the population experience τ replication events. At each event, two locations in the population were randomly chosen. If location i already contained a string, it was copied to site j with probability $P_{ij} = \frac{1}{1 + \exp(-\Delta f_{ij}/T)}$ that depends on the fitness difference $\Delta f_{ij} = f_i - f_j$ between strings $\boldsymbol{S}_i$ and $\boldsymbol{S}_j$ (if site j is empty, $f_j = 0$). T is the Boltzman temperature, which is a measure of the noise tied to replication events, and it was fixed to $T = 0.2$. The fitness of a given string, $\boldsymbol{S}_k$, was obtained from the binary composition of the 10 loci. We considered four types of deleterious fitness landscapes: the standard additive, antagonistic, and synergistic ones plus one in which mutations in the bits representing the 10 viral cistrons were considered lethal. For the three deleterious landscapes we computed the fitness as $f_k = 1 - d_H^{\xi}/10$, where d_H is the Hamming distance (i.e., how many different bits we had) between sequence k and the corresponding loci of the WT genome. ξ measures the sign and strength of epistasis, where ξ equals 1 if additive, ξ is <1 if antagonistic, and ξ is >1 if synergistic (42). During replication, each bit of the amiR159-HCPro target can mutate with the probability μ. The other 10 loci of the strings mutate with the probability $\mu_{l_i} = 3\mu v/2l_i$, where l_i is the length of locus i and the 2/3 is introduced to consider, as a first approximation, that mutations at the third codon positions are neutral. This correction was done to ensure that all loci mutated proportionally to their length. In order to differentiate between the experiments carried out with WT plants and those carried out with 10-4 *A. thaliana* plants, we considered that if the string chosen for replication was the WT genome, it would be degraded with probability $\varepsilon = 0$ for simulations in WT plants and $\varepsilon > 0$ for simulations in 10-4 plants.

As mentioned above, for each lineage we let the population evolve over τ replication events according to the above-described rules. We then took two random samples of size N (Fig. 1B). The first sample was used to initiate the next population (simulating the next passage in the experimental evolutionary lineages) until resistance was broken. The second sample was used to evaluate the likelihood of resistance breaking as follows. For each string $\boldsymbol{S}_i$ in the second sample, we evaluated its pathogenicity as $\theta(\mathbf{S}_i) = 1 - \prod_{k=1}^{21}[1 - \lambda(S_{ik})]$, with $\lambda(S_{ik})$ being the empirical probability that a change in position k of the 21-nt target will be an escape mutation (frequency data from Fig. 4 were corrected by using the Laplace estimator). Next, we evaluated the likelihood of resistance breaking for this second sample after 20 trials (the number of plants inoculated during the challenging experiments) as $P_b = 1 - (1 - \langle p \rangle)^{20}$, where $\langle p \rangle = \frac{1}{N}\sum_{i=1}^{N\theta}(\mathbf{S}_i)$ is the average pathogenicity of all the strains contained in the sample. If P_b was ≥0.05, we assumed that resistance was broken.

For a sample of 20 plants, this threshold means that at least one plant became symptomatic.

Data fitting and parameter inference. To fit the experimental data to the simulation model and to infer relevant population parameters, we used an optimization algorithm (OA) (33) that systematically searched the parameter space defined by $C = \{\tau, \mu, N, \xi, \varepsilon\}$ as follows. First, we defined a starting population of 150 parameter sets, $C_1(0), C_2(0), \ldots, C_{150}(0)$. The parameter values for each one of these $C_h(0)$ parameter sets was randomly assigned within the following ranges: $1 \leq \tau \leq 10^5$, $1 \leq N \leq N_{max}$, $10^{-7} \leq \mu \leq 10^{-3}$, $0.2 \leq \xi \leq 1.8$, and $0.1 \leq \varepsilon \leq 0.5$. For each one of these parameter sets, we ran the simulation algorithm described in the two previous paragraphs. At the end of each simulation we compared the observed cumulative frequencies at passage j shown in Fig. 3, $\rho_{obs}(j)$, with those obtained in the simulation, $\rho_i(j)$, using the equation $d_h = \sum_{j=1}^{28} |\rho_h(j) - \rho_{obs}(j)|$, which represents a distance value between the empirical and the simulated data. This procedure generated a vector of 150 d_h values between the observed and simulated data. We computed then the average distance, $D = \frac{1}{150}\sum_{h=1}^{150} d_h$, from all the 150 parameter sets and chose those sets with a distance smaller than D as a starting point for the next iteration of the OA, $C_i(1)$. Since fewer than 150 parameter sets were left for the next iteration, the rest of the sets were generated by the addition of small perturbations to the retained parameter sets. The whole process was repeated until no change was observed for $\langle d(t) \rangle$ after t iterations of the OA. Notice that for WT plants, $C = \{\tau, \mu, N, \xi\}$, since amiR-mediated degradation was fixed to $\varepsilon = 0$.

RESULTS

***A. thaliana* lines 10-4 and 12-4 differ in amiR159-HCPro expression and susceptibility to TuMV infection.** First, we evaluated whether TuMV had the same level of pathogenicity, p, in both *A. thaliana* transgenic lines 10-4 and 12-4. All plants were inoculated at Boyes' stage 1.03 (i.e., when three rosette leaves are greater than 1 mm in length) (6) and with TuMV infectious sap applied by gentle abrasion onto leaves of the same position on the plant. None of the 30 inoculated 12-4 plants developed symptoms of infection at 14 dpi ($P = 0.000 \pm 0.048$ [±95% confidence interval {CI}, computed by using the Wald adjusted method]). In sharp contrast, 152 out of 218 inoculated 10-4 plants developed obvious symptoms after the same period of time ($P = 0.697 \pm 0.063$). The difference between the results obtained from 10-4 plants and those obtained from 12-4 plants was highly significant ($P < 0.001$ by Fisher's exact test). Significantly, TuMV pathogenicity in 10-4 plants was only 11.80% lower than that in the fully susceptible WT plants (166 out of 210; $P = 0.791 \pm 0.057$), although this small difference was still statistically significant ($P = 0.035$ by Fisher's exact test).

To elucidate the difference in pathogenicities between the two transgenic lines, we first evaluated whether there was any difference in the overall accumulation of amiR159-HCPro. To this end, we analyzed the concentration of the amiR accumulated in sets of each transgenic line at Boyes' stage 1.03 (the developmental stage at which the above-described pathogenicity tests were performed) by RT-qPCR. Twelve 12-4 plants and 11 10-4 plants were analyzed; three independent quantifications were obtained for each plant. The data were analyzed by using a general linear model (GLM), using "plant genotype" as the main random factor and "plant replicate" nested within the plant genotype. This analysis showed that significant heterogeneity exists among plants of the same genotype ($\chi^2 = 264.698$; 21 df; $P < 0.001$). Despite this heterogeneity, the differences among genotypes were highly significant ($\chi^2 = 389.442$; 2 df; $P < 0.001$). On average, 12-4 plants accumulated 111.367 ± 6.998 pg amiR159-HCPro per mg of plant tissue (here errors represent ±1 standard error of the mean [SEM]), whereas 10-4 plants accumulated 4.961 ± 1.370 pg/mg (i.e., 22.45-fold less than 12-4 plants).

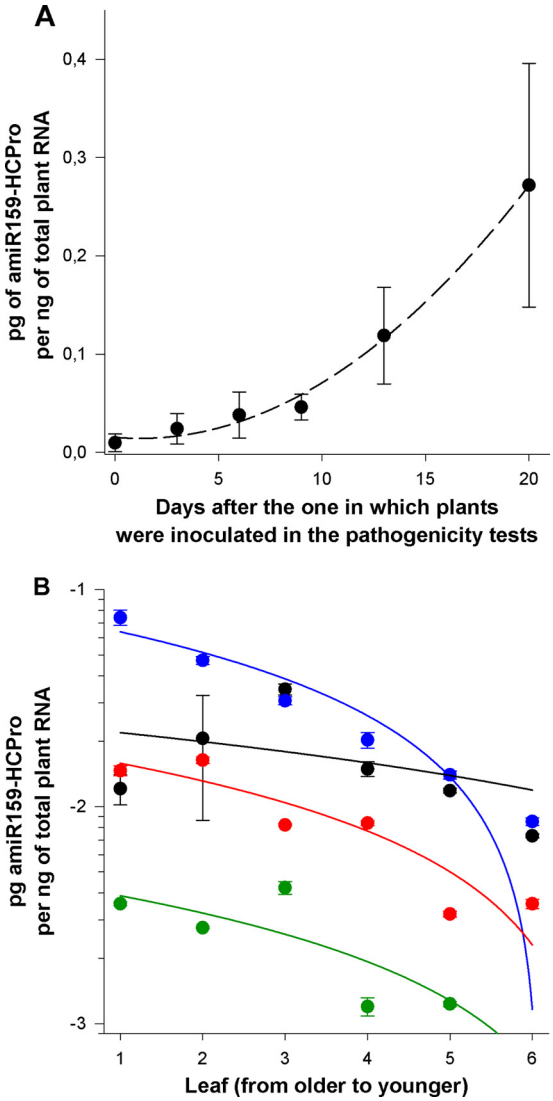

FIG. 2. Pattern of amiR159-HCPro accumulation in the partially resistant transgenic lineage 10-4. (A) Curve of amiR159-HCPro accumulation in the leaf inoculated in the pathogenicity tests (units of picograms of amiR159-HCPro per nanogram of total plant RNA). The dashed line represents the fit to a two-parameter exponential growth model ($R^2 = 0.990$; $F_{1,4} = 405.167$; $P < 0.001$). (B) Pattern of amiR159-HCPro accumulation in six leaves that differ in their developmental stages from four different plants (units of amiR159-HCPro molecules per nanogram of total plant RNA). Each plant is represented by a different color. In all cases, error bars represent ±1 SEM.

Second, we characterized the temporal pattern of the accumulation of amiR159-HCPro in 10-4 leaves whose developmental stage was equivalent to the developmental stage of those inoculated in the pathogenicity tests (e.g., the zero in the ordinate corresponds to Boyes' stage 1.03). Four independent 10-4 plants were analyzed at each time point, and the estimates were averaged among plants. Figure 2A shows that the amount of amiR159-HCPro accumulated per nanogram of plant total RNA increased in a nonlinear fashion as a leaf developed. Indeed, during the first days of the experiment the increase in

the amiR159-HCPro concentration was minor, but accumulation significantly accelerated 10 days after the beginning of the experiment (i.e., accumulation was not linear but exponential) (Fig. 2A).

Third, we looked for differences in the amounts of amiR159-HCPro on different leaves of the same plants (at Boyes' stage 1.06; i.e., six rosette leaves are greater than 1 mm) to see whether this accumulation pattern was consistent among plants. To do so, we estimated the concentration of the amiR in each of six leaves from four different plants. Figure 2B shows the observed pattern of amiR159-HCPro accumulation. A GLM model in which "plant" was treated as a random factor and "leaf" was treated as a covariable highlighted several interesting results. First, the amounts of amiR159-HCPro significantly varied among leaves at different developmental stages, significantly increasing as leaves became older ($\chi^2 = 88.713$; 1 df; $P < 0.001$). Second, in agreement with data from our first test, plants were heterogeneous in their average amounts of accumulated amiR159-HCPro ($\chi^2 = 497.603$; 4 df; $P < 0.001$). Third, differences existed among plants in the rate at which the concentration of amiR159-HCPro increased ($\chi^2 = 96.531$; 3 df; $P < 0.001$ [test for homogeneity of slopes]). In other words, early stochastic events during development determined the initial amount of amiR159-HCPro that would characterize a leaf, and these differences were further amplified as leaves expanded and developed.

Therefore, all these analyses led to the conclusion that the transgenic line 10-4 shows incomplete genetic penetrance (i.e., not all individual transgenic plants are resistant) and variable gene expressivity for resistance (i.e., not all resistant individuals express amiR159-HCPro at the same level). In contrast, line 12-4 showed a complete genetic penetrance of the resistance trait. These phenotypic differences are due to differences in the amount and timing of expression of amiR159-HCPro. Rather than being an issue, we will take full advantage of the 10-4 peculiarity to evaluate the effect of evolving TuMV populations on the subinhibitory and variable expression of amiR159-HCPro.

Resistance breaking in TuMV populations evolving in WT *A. thaliana* plants at the mutation-drift balance. We aimed to evaluate the likelihood that TuMV populations replicating and evolving in fully susceptible WT *A. thaliana* hosts contained escape mutants able to overcome the resistance mediated by amiR159-HCPro. To this end, 25 independent evolution lineages were founded by inoculating WT *A. thaliana* plants with sap obtained from a pool of *N. benthamiana* plants previously inoculated with an infectious TuMV cDNA genome. Therefore, the amount of genetic variability in the inoculum will not be zero but the lowest amount technically possible. All plants were inoculated with the same amount of this infectious sap. All plants became infected, as confirmed by the presence of symptoms. Every 14 dpi, infected plants were sampled; one portion of the sample was used to inoculate the following set of plants, another portion was stored for future analyses, and a third portion was used to challenge 20 12-4 transgenic plants per evolving lineage (total, $20 \times 25 = 500$ plants per challenge experiment) (Fig. 1). The pathogenicity of each evolving lineage at each passage was evaluated by an inspection of symptoms; a lineage was considered capable of breaking resistance if it was able to infect at least one 12-4 plant in the challenge

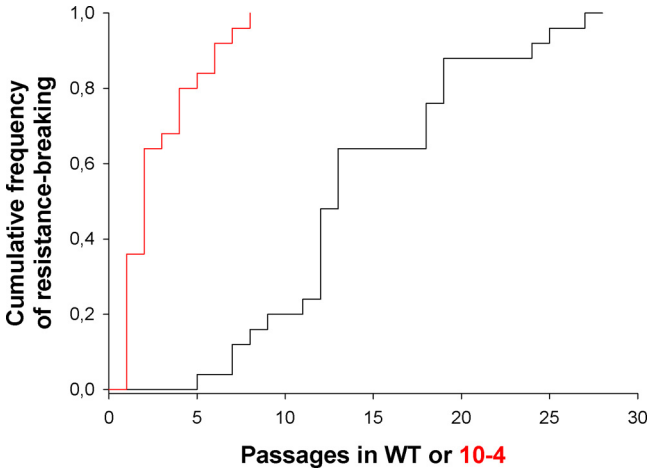

FIG. 3. Cumulative frequency of lineages capable of escaping from amiR159-HCPro resistance. The black line corresponds to the lineages evolved in WT *A. thaliana* plants. The red line corresponds to the lineages evolved in partially resistant *A. thaliana* 10-4 plants. The ability of evolving TuMV populations to escape from amiR159-HCPro was evaluated in 12-4 plants that were fully resistant to the ancestral TuMV genotype. A population was considered to be able to escape from resistance when at least one 12-4 plant was infected.

experiments (i.e., pathogenicity of ≥ 0.05). We hypothesized that mutants in the amiR159-HCPro target would arise and stay in the population at the mutation-drift balance and that they would be transferred to the 12-4 plants during challenge in a rather stochastic manner. The black line in Fig. 3 shows the cumulative frequency of lineages that overcame resistance at each passage. The first break out occurred at passage 6, and all 25 lineages were capable of breaking resistance after 28 passages. A Kaplan-Meier regression showed that the median time for resistance breaking was 14.000 ± 0.480 passages in WT *A. thaliana* plants.

Resistance breaking in TuMV populations evolving in partially susceptible *A. thaliana* 10-4 plants. Next, we sought to evaluate the effect that TuMV replication under subinhibitory concentrations of amiR159-HCPro had on resistance durability. To this end, we repeated the evolution experiment by performing serial passages in partially resistant *A. thaliana* 10-4 plants; all other operations were kept identical. We reasoned that in this case, the TuMV populations infecting plants would be under the selective pressure imposed by the presence of the amiR in the cells but at concentrations that may still allow viral replication. We predicted that in such a situation, escape mutations would have a selective advantage and accumulate in the population at the mutation-selection-drift balance, at frequencies higher than those in the previous experiment. This would allow a faster resistance breaking after challenge of the 12-4 plants. The red line in Fig. 3 illustrates the time course accumulation of lineages able to break the resistance. As we predicted, lineages broke resistance faster than in the previous experiment, with many of them already containing escape mutants after the first passage and all 25 being able to do so after only eight passages. A Kaplan-Meier regression showed that in this case, the median time for resistance breaking was 2.000 ± 0.343 passages in 10-4 plants, a value that is significantly lower

TABLE 1. Escape alleles found in the TuMV populations evolved in fully susceptible WT *A. thaliana* plants

Allele (sequence)[a]	Lineage(s) (passage)[b]	Type of mutation[c]
WT (ACA GUC GAG UGC GUG AGC AAG UUA)	Ancestral WT	
1 (ACA GUC GAG UG**U** GUG AGC AAG UUA)	12 (6), 18 (9), 9 (13), 7 (14), 19 (14), 21 (14), 20 (19)	Synonymous
2 (ACA GUC GAG UGC **A**UG AGC AAG UUA)	10 (10), 3 (14), 8 (14), 22 (14), 24 (14), 4 (19), 16 (20)	V→M
3 (ACA GUC GAG UG**U** GUG AGC AA**N** UUA)	6 (14), 11 (27), 23 (27)	Synonymous/synonymous or K→N
4 (ACA GUC GAG UGC GUG AG**U** AAG UUA)	14 (13), 1 (27)	Synonymous
5 (ACA GUC **A**AG UGC GU**A** AGC AAG UUA)	15 (8)	E→K/synonymous
6 (ACA GUC GAG UGC GUG **G**G**U** AAG UUA)	25 (8)	S→G
7 (ACA GUC G**UA** UGC GUG AGC AAG UUA)	13 (14)	E→V
8 (ACA GUC GAG UGC GUG AGC A**G**G UUA)	5 (18)	K→R
9 (ACA **A**UC **A**AG UGC GUG AGC AAG UUA)	2 (20)	V→I/E→K
10 (ACA GUC GAG UGC GUG AGC **G**AG UUA)	17 (20)	K→E

[a] The 21 nt of the target is underlined. The mutated sites are shown in boldface type.
[b] The lineage (and passage) in which each allele was observed is indicated.
[c] Indicates whether the mutations were synonymous or involved an amino acid replacement.

than that obtained for the 12-4-evolved lineages ($\chi^2 = 54.971$; 1 df; $P < 0.001$ [by a Mantel-Cox test]).

Changes in the amiR159-HCPro target. After determining that a TuMV lineage was capable of escaping from amiR159-HCPro-mediated resistance, we sought to characterize the genetic changes associated with its new phenotype. Based on results reported previously by Lin et al. with TuMV (31), supported by previous accumulated knowledge from HIV-1 (4, 17, 48–52) and poliovirus (23) cell culture experiments, we hypothesized that in all cases, the dominant TuMV genotype in the infected 12-4 plants after challenge would carry at least one mutation in the target sequence. To test this expectation, we obtained the 21-nt target consensus sequence for the viral population replicating in each 12-4 plant. Tables 1 and 2 show the different escape alleles found in TuMV populations evolving in WT *A. thaliana* and 10-4 plants, respectively. Regarding Table 1, a total of 10 different alleles were characterized, although four of them (alleles 1, 2, 3, and 4) were pervasively seen in more than one lineage, a clear example of convergent evolution. The two most common nucleotide substitutions were a synonymous one at target site 11 (in 10 cases) and a nonsynonymous one at position 12 (in 7 instances), which gave rise to a conservative amino acid replacement, V to M, in the HC-Pro protein. Half of the alleles contained a single substitution (alleles 1, 2, 4, 8, and 10), whereas the other half contained two mutations. Four of these substitutions were synonymous, and eight were associated with amino acid replacements. Interestingly, lineages 6, 11, and 23 all showed a polymorphism at position 20 of the target. In all three cases one of the coexisting alleles was a synonymous substitution, whereas the other one involved a conservative amino acid replacement, K to N, in HC-Pro.

Regarding Table 2, seven escape alleles were identified in the TuMV populations evolved in the partially resistant 10-4 plants. Four of them were not observed for the populations evolving in WT *A. thaliana* plants (alleles 11, 12, 13, and 14), although only one of the mutations in these alleles was not previously observed (the A-to-C nonsynonymous change at position 19 of allele 11). The two most common alleles in this experiment were also those observed in the first experiment (alleles 1 and 2): the synonymous substitution at position 11 of the target (in 12 cases) and the second most abundant one, the nonsynonymous replacement at site 12 (in 8 cases).

Pooling data from both experiments, 52 of the 55 observed mutations were transitions, with G-to-A and C-to-U changes dominating the mutational spectrum. Consistent with the principle that transitions are biochemically more likely to occur than transversions, the maximum composite likelihood estimate of the overall transition-to-transversion rate ratio is 14.176. This excess also occurs when purines (ratio, 20.599) and pyrimidines (ratio, 40.639) are considered separately. It is well known that viral coding regions show an excess of transitions over transversions (9, 26, 31, 43). Three reasons can account for this bias: (i) the underlying mechanisms of mutation render transitions easier than transversions, (ii) the redundancy of the genetic code is expected to make the average

TABLE 2. Escape alleles found in TuMV populations evolved in partially resistant 10-4 plants

Allele (sequence)[a]	Lineage(s) (passage)	Type of mutation
WT (ACA GUC GAG UGC GUG AGC AAG UUA)	Ancestral WT	
1 (ACA GUC GAG UG**U** GUG AGC AAG UUA)	3 (1), 6 (1), 8 (1), 13 (1), 15 (1), 14 (2), 21 (2), 25 (2), 7 (4), 11 (4), 22 (5)	Synonymous
2 (ACA GUC GAG UGC **A**UG AGC AAG UUA)	2 (1), 9 (1), 17 (2), 10 (3), 4 (4), 18 (6), 24 (7), 20 (8)	V→M
4 (ACA GUC GAG UGC GUG AG**U** AAG UUA)	23 (2)	Synonymous
11 (ACA GUC GAG UGC GUG AGC **A**C**G** UUA)	1 (2), 19 (6)	K→T
12 (ACA GUC **A**AG UG**U** GUG AGC AAG UUA)	5 (1)	E→K/synonymous
13 (ACA **A**UC GAG UGC GUG AGC AAG UUA)	16 (1)	V→I
14 (ACA GUC **A**AG UGC GUG AGC AAG UUA)	12 (2)	E→K

[a] The 21 nt of the target is underlined. The mutated sites are shown in boldface type.

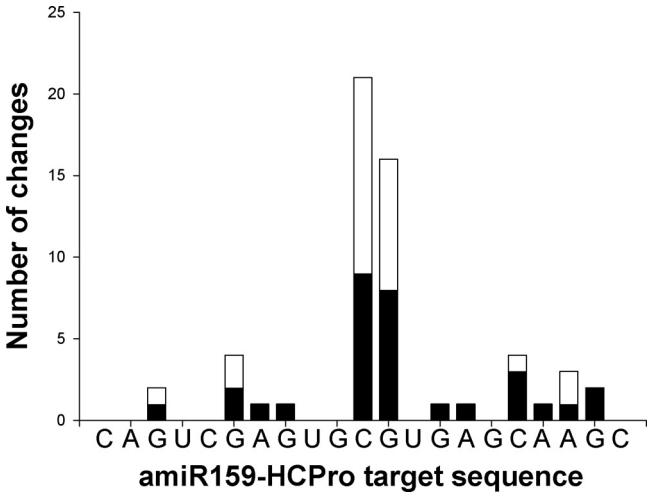

FIG. 4. Distribution of mutations in escape viruses along the amiR159-HCPro target sequence. Black bars correspond to the frequency of mutations that arose in WT *A. thaliana* plants; white bars correspond to those observed for the 10-4 transgenic line.

effect of transitions smaller than that of transversions, and (iii) RNA editing by deaminase-like enzymes has been shown to induce transition mutations in single-stranded regions of certain viral genomes (3).

Convergent evolution would imply that the frequency distribution of changes along the 21-nt target should be similar in both experiments. Figure 4 shows these distributions for both types of TuMV populations. A homogeneity test detected no differences among both pattern distributions ($\chi^2 = 8.388$; 11 df; $P = 0.678$), thus supporting the notion of widespread convergent evolution, likely driven by the selective advantage of mutations at sites 11 and 12 of the target.

Estimates of population genetic parameters by *in silico* simulations. To provide new insights into the above-described results as well as to evaluate the range of population parameters compatible with our observations, we simulated the two evolution experiments by using digital viral genomes replicating, mutating, and being subjected to transmission bottlenecks as in the experiments described above (Fig. 1B and see Materials and Methods). We performed a search of parameter space using an optimization algorithm (OA) to find a set of parameters that minimized the distance between the data shown in Fig. 3 and those simulated. For the simulations of the evolution experiments carried out with WT *A. thaliana* plants (i.e., without sequence-specific degradation), we analyzed a total of 393 runs of the OA: 129 runs assuming that mutations had additive effects, 210 runs assuming that they interacted epistatically, and 54 runs assuming that mutations outside the target and affecting other genes were lethal. Each run of the OA consisted of 400 generations, with a population of parameter sets of 150, resulting in more than 25 million simulations. The parameter set that generated the lowest and more robust distance ($d = 0.56$; $R^2 = 0.976$; $F_{1,27} = 1{,}114.571$; $P < 0.001$) between the experiments and the simulation model was obtained with the additive fitness landscape with the following parameters: $\langle\tau\rangle = 13{,}918.23 \pm 75.64$ viral replications between passages, $\langle\mu\rangle = (4.11 \pm 0.33) \times 10^{-5}$ mutations per site and generation, and $\langle N_e\rangle = 956.89 \pm 23.76$ digital viruses transmitted per bottleneck event (i.e., ~19% of the total population). Figure 5A shows the results of the simulation obtained with this set of parameters. The simulated values of the frequency of lineages escaping from amiR159-HCPro are shown with red dots on top of the black line that represents the experimental data.

For the evolution experiments in the partially resistant 10-4 plants (i.e., with sequence-specific degradation), we followed the same procedure, although we restricted the study to only the additive fitness landscape (that gave the best fit for the WT plants) and added a degradation rate, $\varepsilon > 0$, to the parameter set. This degradation rate simulated the assumption that 10-4 plants expressed amiR159-HCPro and that, hence, the silencing machinery may still be capable of degrading a fraction of the viral population (i.e., the strings containing a WT target sequence are degraded with probability ε [see Materials and Methods]). For this case, we ran 150 replicas of the OA, thus exploring a total of 6 million simulations. Among all these simulations, the parameter combination providing the smallest distance between experimental and simulated data ($d = 0.16$; $R^2 = 0.995$; $F_{1,7} = 733.253$; $P < 0.001$) was as follows: $\langle\tau\rangle = 5{,}629.51 \pm 63.79$, $\langle\mu\rangle = (7.69 \pm 1.12) \times 10^{-5}$, $\langle N_e\rangle = 68.61 \pm 11.78$ (i.e., ~1.4% of the potential maximum population size), and $\langle\varepsilon\rangle = 0.223 \pm 0.098$ per genome. The best fit to the exper-

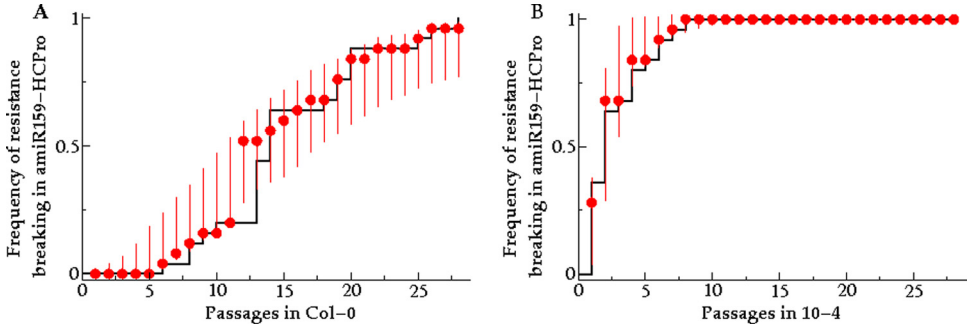

FIG. 5. Results of the simulation studies for the set of parameters that showed the best fit to data shown in Fig. 3. (A) Simulation results for the WT *A. thaliana*-evolved TuMV lineages. (B) Simulation results for the TuMV lineages evolved in partially resistant 10-4 plants. The red dots correspond to the best-fitting trajectory obtained from the most optimized parameter set. Red bars indicate the standard deviations among 10^3 runs of the simulation model using the best-fitting parameters.

imental data is shown in Fig. 5B. As described above, the red dots represent the simulated values for this parameter set. Not surprisingly, the mutation rates estimated for both experiments are on the same order of magnitude and close to the only experimental value reported previously for potyviruses (43).

The degradation of genomes containing nonmutated amiR159-HCPro targets in 10-4 plants has two interlinked effects. First, there was a reduction of 92.83% in $\langle N_e \rangle$: not all genomes contained in the inoculum were capable of replicating in the partially susceptible plants, and a certain fraction was degraded. Second, we expected an apparent reduction in the number of viral replication events supported by the two plant genotypes. In Col-0 plants all the viral progeny produced may eventually contribute to future replications. On the other hand, in 10-4 plants, we expected part of the progeny to be degraded by the amiRs and, hence, not contribute to future replications. The model catches this expectation and shows that 10-4 plants supported ~2.5-times-fewer replication events than the WT plants. Consistently, the viral populations replicating in 10-4 plants did not reach carrying capacity, and therefore, the number of genomes transmitted to the next infection cycle was 13.95-fold lower. This reduction in the size of the transmitted population enhances the effect of genetic drift in the 10-4 lineages. That being said, it is important to recall that two different evolutionary regimes are in play for each plant genotype. In the fully susceptible WT plants, purifying selection and drift should be the only factors affecting allele frequencies, since mutations in the target would be either deleterious or neutral; deleterious alleles will not reach high frequencies. The time to fixation of a neutral allele whose initial frequency is negligible is $4\langle N_e \rangle = 3{,}827.56$ generations (27), which is less than the estimated number of viral replications, $\langle \tau \rangle$, thus making it likely that some neutral alleles in the target would drift to high frequencies in the population. In contrast, in partially resistant 10-4 plants, positive selection also enters the picture, since escape alleles will clearly be beneficial in the presence of amiR159-HCPro. Indeed, we estimate that the average selection coefficient for such a beneficial allele to survive drift should be $\langle s \rangle > 1/\langle N_e \rangle = 0.015$ (27), a low value that ensures that many mutations conferring resistance will survive drift.

Finally, the mutation rates estimated for both experiments are in the range of 4×10^{-5} to 8×10^{-5} mutations per site, values that are very close to recent estimates obtained for another potyvirus, *Tobacco etch virus* (41, 43), and, more generally, for other plant viruses (33, 41). This excellent agreement gives support to the validity of our modeling approach as well as to the conclusions derived from it.

DISCUSSION

The long-term effectiveness of genetic resistances to plant viruses is constantly being challenged by the evolutionary potential of RNA viruses (21), creating the necessity for the development of new resistance strategies. In the early 1990s it was recognized that the transgenic expression of virus-derived sequences resulted in a highly efficient defense against plant viruses (32), with this defense being mediated by the posttranscriptional degradation of RNA genomes guided by virus-derived small interfering RNAs (siRNAs) (25). In recent years, plants that are resistant to virus infection have been engineered by use of this approach (11, 18, 29, 36, 49). However, the transgenic expression of long viral sequences raises biosafety concerns regarding the possibility of recombination and the generation of new and potentially virulent strains (44). Taking advantage of the functional similarities between siRNA and miRNAs, Niu et al. (38) modified the backbone of *A. thaliana* pre-miRNA159, replacing it with short 21-nt viral sequences, resulting in highly specific resistant plants. This approach has at least two advantages compared with the expression of long viral sequences. First, it should have fewer off-target effects, as the amiR sequences are shorter than those required for homology-dependent gene silencing. Second, recombination is not a concern anymore, given the shortness of the amiRs. However, this approach may still raise a major concern: the high mutability of RNA viruses makes it likely that resistant virus variants will emerge, as already observed in *in vitro* experiments with mammalian viruses (4, 12, 17, 22, 23, 30, 40, 48, 52). The objective of the present work was to evaluate the likelihood of the emergence of such escape variants in viral populations replicating in fully susceptible reservoir plants as well as in plants expressing resistance at subinhibitory levels. Toward accomplishing this objective, we have performed two different evolution experiments using the pathosystem TuMV/*A. thaliana*, together with *in silico* computational models simulating both evolution experiments. The first experiment was designed to mimic a situation in which crops of resistant transgenic plants coexisted with crops of fully susceptible ones that acted as virus reservoirs. In this case, we observed an increase in the number of evolving lineages that were capable of successfully infecting the fully resistant host. Such escape mutants should most likely be neutral, or perhaps even slightly deleterious, maintained by complementation, in the evolving population. Our second experiment was aimed at mimicking a situation in which the expression level of the antiviral amiR was variable among plants, with some of them having suboptimal levels that allow virus replication and the selection of escape variants. In the second case we found that these populations accumulated escape mutations at a much higher frequency and, therefore, were able to successfully infect the fully resistant hosts at earlier times in virus evolution. The second result was highly predictable, since it recapitulates the evolution of bacteria at antibiotic concentrations below the MIC (14) and has been solidly established. At subinhibitory concentrations of the antiviral amiR, mutant genotypes gain a fitness advantage, given their ability to replicate despite the presence of the antiviral amiR, whereas wild-type genomes may still suffer from the inhibitory effects. This fitness advantage results in the accumulation of escape alleles above what was expected from the first experiment.

In all 50 cases, the molecular characterization of the escape mutants confirmed the presence of mutations in the amiR159-HCPro target. In agreement with the mutant spectra described previously for other viruses, including TuMV, we have observed an excess of transition mutations (9, 26, 31, 43). Particularly interesting is the fact that G-to-A and C-to-U transitions represented 95% of all mutations observed. These transitions are from the particular type induced by cellular cytidine deaminases involved in innate immune responses to viral infection (13), a phenomenon particularly well described for HIV-1 and other retroviruses (16) but hitherto not described for RNA

viruses. This observation is in good agreement with those described previously Lin et al. (31), thus giving additional support to the hypothesis that as an antiviral strategy, plants may have an RNA-editing system that induces hypermutagenesis in viral genomes. We note that *A. thaliana* contains a family of nine paralogous genes that have been annotated cytidine deaminases owing to their homology to the *CDA1* locus (47).

Indeed, mutations were unevenly distributed along the 21-nt target and concentrated mainly at positions 11 and 12, in a clear case of convergent evolution at the molecular level. Convergent evolution is a widespread phenomenon in RNA viruses both in experimental (8, 15, 53) and in natural (5, 35) populations. Although these convergences could in principle be explained from a neutralist point of view as resulting from mutational bias, it is more likely that parallel and convergent substitutions are adaptive. This pattern would result from viruses facing identical selective pressures, with few alternative adaptive pathways, as expected for their simple and compacted genomes. In agreement with our observation, Lin et al. (31) classified position 11 as being moderately crucial and position 12 as being critical for resistance breaking, although other sites qualified as being crucial did not show a high frequency of variation in our experiments. In contrast to the study by Lin et al. (31), in which the targeted sequence was neutral to the virus, here amiR159-HCPro targeted a coding region of the TuMV HC-Pro cistron, and consequently, mutations in escape variants must result form the balance between avoiding recognition by amiR159-HCPro and retaining biological function. Indeed, this coding effect may explain why Lin et al. observed an excess of critical positions at the 5′ end of the amiR. Additionally, a potential explanation for convergence in these two central sites relies on the fact that imperfect pairing with central mismatches in small RNA-target hybrids promotes translational repression as it excludes slicing (7). This observation suggests the possibility that imperfect pairing between the amiR and mutated targets might lead to translational repression rather than viral RNA cleavage. In contrast to the catalytic effects of amiR-mediated viral RNA cleavage, translational repression requires stoichiometric amounts of amiRs and therefore is not as efficient. Inefficient translation inhibition might allow residual viral replication, and progeny virus can still escape repression by fixing changes in the target sequence.

All in all, our results suggest that the durability of amiR-based resistance may be too short in time to make it a profitable approach. However, this assertion has to be carefully considered in the context that we designed our experiments in such a way that they represent the most favorable possible situation for resistance breaking. For instance, our challenge experiments were done with inocula that represent 1 to 20% of the whole viral population, according to our simulations. In a natural situation in the field, transmission would be mediated by vectors, which impose more dramatic bottlenecks, in the order of units per vector and transmission event (1, 2, 37), thus minimizing the likelihood of the transmission of very-low-frequency escape alleles, although large vector populations will contribute to an increase of the chances of transmission. Furthermore, the way in which we sampled viral populations, homogenizing the whole plant, provided transmission probability for all genomes present in the plant. The spatial structure imposed by the plant architecture limits gene flow among distal parts of the plant, up to the point that each part may be dominated by different viral genotypes (28). This means that variants may not reach a high frequency within the whole metapopulation despite having some local fitness advantage. Therefore, by feeding on particular leaves, vectors would miss loading escape mutants that may be abundant in other parts of the plant. All these factors, plus surely some additional ones, increase the stochasticity of escape alleles spilling over from their reservoirs to the amiR transgenic crops, thus perhaps increasing resistance durability. Another factor that may affect durability, as suggested by our results, is the level at which the amiR is expressed. We have shown that subinhibitory expression levels would indeed select for resistance alleles, facilitating their spread in transgenic populations. This adds a cautionary note for biotechnologists when selecting their new transgenic plants. Another way of increasing the resistance durability could be to express more than one amiR in a transgenic crop, to target different highly conserved RNA sequences in the viral genome, or to combine amiR-mediated resistance with other genetic resistances. By combining multiple amiRs into a single plant, the likelihood of resistance breaking will drop exponentially. Currently, we are exploring this possibility in the laboratory.

ACKNOWLEDGMENTS

We thank S. D. Yeh for kindly providing p35STuMV and J. Forment for technical computational assistance.

This work was supported by Human Frontiers Science Program Organization grant RGP12/2008, Generalitat Valenciana grant PROMETEO/2010/019, and CSIC grant 2010TW0015. We also acknowledge support from The Santa Fe Institute.

REFERENCES

1. **Ali, A., et al.** 2006. Analysis of genetic bottlenecks during horizontal transmission of *Cucumber mosaic virus*. J. Virol. **80:**8345–8350.
2. **Betancourt, M., A. Fereres, A. Fraile, and F. García-Arenal.** 2008. Estimation of the effective number of founders that initiate an infection after aphid transmission of a multipartite plant virus. J. Virol. **82:**12416–12421.
3. **Bishop, K. N., R. K. Holmes, A. M. Sheehy, and M. H. Malim.** 2004. APOBEC-mediated editing of viral RNA. Science **305:**645.
4. **Boden, D., O. Pusch, F. Lee, L. Tucker, and B. Ramratnam.** 2003. Human immunodeficiency virus type 1 escape from RNA interference. J. Virol. **77:**11531–11535.
5. **Boucher, C. A., et al.** 1992. Ordered appearance of zidovudine resistance mutations during treatment of 18 human immunodeficiency virus-positive subjects. J. Infect. Dis. **165:**105–110.
6. **Boyes, D. C., et al.** 2001. Growth stage-based phenotypic analysis of *Arabidopsis*: a model for high throughput functional genomics in plants. Plant Cell **13:**1499–1510.
7. **Brodersen, P., et al.** 2008. Widespread translational inhibition by plant miRNAs and siRNAs. Science **320:**1185–1190.
8. **Bull, J. J., et al.** 1997. Exceptional convergent evolution in a virus. Genetics **147:**1497–1507.
9. **Burch, C. L., S. Gudayer, D. Samarov, and H. Shen.** 2007. Experimental estimates of the abundance and effects of nearly neutral mutations in the RNA virus ϕ6. Genetics **176:**467–476.
10. **Chen, C. C., et al.** 2003. Identification of *Turnip mosaic virus* isolates causing yellow stripe and spot on calla lily. Plant Dis. **87:**901–905.
11. **Chen, Y. K., D. Lohuis, R. Goldbach, and M. Prins.** 2004. High frequency induction of RNA-mediated resistance against *Cucumber mosaic virus* using inverted repeat constructs. Mol. Breed. **14:**215–226.
12. **Coburn, G. A., and B. R. Cullen.** 2002. Potent and specific inhibition of human immunodeficiency virus type 1 replication by RNA interference. J. Virol. **76:**9225–9231.
13. **Conticello, S. G., C. J. Thomas, S. K. Petersen-Mahrt, and M. S. Neuberger.** 2005. Evolution of the AID/APOBEC family of polynucleotide (deoxy)cytidine deaminases. Mol. Biol. Evol. **22:**367–377.
14. **Couce, A., and J. Blázquez.** 2009. Side effects of antibiotics on genetic variability. FEMS Microbiol. Rev. **33:**531–538.
15. **Cuevas, J. M., S. F. Elena, and A. Moya.** 2002. Molecular basis of adaptive convergence in experimental populations of RNA viruses. Genetics **162:**533–542.

16. **Cullen, B. R.** 2006. Role and mechanism of action of the APOBEC3 family of antiretroviral resistance factors. J. Virol. **80:**1067–1076.
17. **Das, A. T., et al.** 2004. Human immunodeficiency virus type 1 escapes from RNA interference-mediated inhibition. J. Virol. **78:**2601–2605.
18. **Di Nicola-Negri, E., A. Brunetti, M. Tavazza, and V. Ilardi.** 2005. Hairpin RNA-mediated silencing of *Plum pox virus* P1 and HC-Pro genes for efficient and predictable resistance to the virus. Transgenic Res. **14:**989–994.
19. **Elbashir, S. M., J. Martínez, A. Patkaniowska, W. Lendeckel, and T. Tuschl.** 2001. Functional anatomy of siRNAs for mediating efficient RNAi in *Drosophila melanogaster* embryo lysate. EMBO J. **20:**6877–6888.
20. **Elena, S. F., R. V. Solé, and J. Sardanyés.** 2010. Simple genomes, complex interactions: epistasis in RNA virus. Chaos **20:**e26106.
21. **García-Arenal, F., and B. A. McDonald.** 2003. An analysis of the durability of resistance to plant viruses. Phytopathology **93:**941–952.
22. **Ge, Q., et al.** 2003. RNA interference of influenza virus production by directly targeting mRNA for degradation and indirectly inhibiting all viral RNA transcription. Proc. Natl. Acad. Sci. U. S. A. **100:**2718–2723.
23. **Gitlin, L., J. K. Stone, and R. Andino.** 2005. Poliovirus escape from RNA interference: short interfering RNA-target recognition and implications for therapeutic approaches. J. Virol. **79:**1027–1035.
24. **Guo, H. S., Q. Xie, J. F. Fei, and N. H. Chua.** 2005. MicroRNA directs mRNA cleavage of the transcription factor NAC1 to downregulate auxin signals for *Arabidopsis* lateral root development. Plant Cell **17:**1376–1386.
25. **Hamilton, A. J., and D. C. Baulcombe.** 1999. A species of small antisense RNA in posttranscriptional gene silencing in plants. Science **286:**950–952.
26. **Haydon, D., N. Knowles, and J. McCauley.** 1998. Methods for the detection of non-random base substitution in virus genes: models of synonymous nucleotide substitution in picornavirus genes. Virus Genes. **16:**253–266.
27. **Hedrick, P. W.** 2004. Genetics of populations, p. 376–379. Jones and Bartlett Publishers, Sudbury, MA.
28. **Jridi, C., J. F. Martin, V. Mareie-Jeanne, G. Labonne, and S. Blanc.** 2006. Distinct viral populations differentiate and evolve independently in a single perennial host plant. J. Virol. **80:**2349–2357.
29. **Kalantidis, K., S. Psaradakis, M. Tabler, and M. Tsagris.** 2002. The occurrence of CMV-specific short RNAs in transgenic tobacco expressing virus-derived double-stranded RNA is indicative of resistance to the virus. Mol. Plant Microb. Interact. **15:**826–833.
30. **Krönke, J., et al.** 2004. Alternative approaches for efficient inhibition of hepatitis C virus RNA replication by small interfering RNAs. J. Virol. **78:** 3436–3446.
31. **Lin, S. S., et al.** 2009. Molecular evolution of a viral non-coding sequence under the selective pressure of amiRNA-mediated silencing. PLoS Pathog. **5:**e1000312.
32. **Lindbo, J. A., and W. G. Dougherty.** 2005. Plant pathology and RNAi: a brief history. Annu. Rev. Phytopathol. **43:**191–204.
33. **Malpica, J. M., et al.** 2002. The rate and character of spontaneous mutation in an RNA virus. Genetics **162:**1505–1511.
34. **Marín, J., and R. V. Solé.** 1999. Macroevolutionary algorithms: a new optimization method on fitness landscapes. IEEE Trans. Evol. Comput. **3:**272–286.
35. **Martínez-Picado, J., et al.** 2000. Antiretroviral resistance during successful therapy of HIV type 1 infection. Proc. Natl. Acad. Sci. U. S. A. **97:**10948–10953.
36. **Missiou, A., et al.** 2004. Generation of transgenic potato plants highly resistant to *Potato virus Y* (PVY) through RNA silencing. Mol. Breed. **14:**185–197.
37. **Moury, B., F. Fabre, and R. Senoussi.** 2007. Estimation of the number of viral particles transmitted by an insect vector. Proc. Natl. Acad. Sci. U. S. A. **45:**17891–17896.
38. **Niu, Q. W., et al.** 2006. Expression of artificial microRNAs in transgenic *Arabidopsis thaliana* confers virus resistance. Nat. Biotechnol. **24:**1420–1428.
39. **Qu, J., J. Ye, and R. Fang.** 2007. Artificial microRNA-mediated virus resistance in plants. J. Virol. **81:**6690–6699.
40. **Sabariegos, R., M. Giménez-Barcons, N. Tàpia, B. Clotet, and M. A. Martínez.** 2006. Sequence homology required by human immunodeficiency virus type 1 to escape from short interfering RNAs. J. Virol. **80:**571–577.
41. **Sanjuán, R., P. Agudelo-Romero, and S. F. Elena.** 2009. Upper-limit mutation rate estimation for a plant RNA virus. Biol. Lett. **5:**394–396.
42. **Sardanyés, J., R. V. Solé, and S. F. Elena.** 2009. Replication mode and landscape topology differentially affect RNA virus mutational load and robustness. J. Virol. **83:**12579–12589.
43. **Tromas, N., and S. F. Elena.** 2010. The rate and spectrum of spontaneous mutations in a plant RNA virus. Genetics **185:**983–989.
44. **Turturro, C., et al.** 2008. Evaluation of potential risks associated with recombination in transgenic plants expressing viral sequences. J. Gen. Virol. **89:**327–335.
45. **Varkonyi-Gasic, E., R. Wu, M. Wood, E. F. Walton, and R. P. Hellens.** 2007. A highly sensitive RT-PCR method for detection and quantification of microRNAs. Plant Methods **3:**12.
46. **Vaucheret, H., F. Vázquez, P. Crete, and D. P. Bartel.** 2004. The action of ARGONAUTE1 in the miRNA pathway and its regulation by the miRNA pathway are crucial for plant development. Genes Dev. **18:**1187–1197.
47. **Vicenzetti, S., et al.** 1999. Cloning, expression, and purification of cytidine deaminase from *Arabidopsis thaliana*. Protein Expr. Purif. **15:**8–15.
48. **Von Eije, K. J., O. ter Brake, and B. Berkhout.** 2008. Human immunodeficiency virus type 1 escape is restricted when conserved genome sequences are targeted by RNA interference. J. Virol. **82:**2895–2903.
49. **Wang, M. B., D. C. Abbot, and P. M. Waterhouse.** 2000. A single copy of a virus-derived transgene encoding hairpin RNA gives immunity to *Barley yellow dwarf virus*. Mol. Plant Pathol. **1:**347–356.
50. **Warthmann, N., H. Chen, S. Ossowski, D. Weigel, and P. Hervé.** 2008. Highly specific gene silencing by artificial microRNAs in rice. PLoS One **3:**e1829.
51. **Westerhout, E. M., and B. Berkhout.** 2007. A systematic analysis of the effect of target RNA structure on RNA interference. Nucleic Acids Res. **35:**4322–4330.
52. **Westerhout, E. M., M. Ooms, M. Vink, A. T. Das, and B. Berkhout.** 2005. HIV-1 can escape from RNA interference by evolving an alternative structure in its RNA genome. Nucleic Acids Res. **33:**796–804.
53. **Wichman, H. A., M. R. Badgett, L. A. Scott, C. M. Boulianne, and J. J. Bull.** 1999. Different trajectories of parallel evolution during viral adaptation. Science **285:**411–424.